Open Access Articles

Neutron Capture by 94,96Zr and the Decays of 97Zr and 97Nb

The Faculty of Oregon State University has made this article openly available.
Please share how this access benefits you. Your story matters.

Citation	Krane, K. S. (2014). Neutron capture by 94,96Zr and the decays of 97Zr and 97Nb. Applied Radiation and Isotopes, 94, 60-66. doi:10.1016/j.apradiso.2014.07.006
DOI	10.1016/j.apradiso.2014.07.006
Publisher	Elsevier
Version	Accepted Manuscript
Terms of Use	http://cdss.library.oregonstate.edu/sa-termsofuse

Neutron Capture by ^{94,96}Zr and the Decays of ^{97}Zr and ^{97}Nb

K. S. Krane

Department of Physics, Oregon State University, Corvallis OR 97331

Cross sections for radiative neutron capture have been determined for ^{94}Zr and ^{96}Zr using the activation technique with samples of naturally occurring Zr metal. The sensitivity to the correction for epithermal neutrons in the determination of small thermal cross sections is discussed, particularly in view of the variation in the resonance integral at different sites in the reactor. Gamma-ray spectroscopic studies of the decays of ^{97}Zr and its daughter ^{97}Nb have been performed, leading to improved values of the energies and intensities of the emitted γ rays, and correspondingly improved values for the energy levels and β feedings of excited states populated in ^{97}Nb and ^{97}Mo.

Keywords: ^{94,96}Zr neutron capture cross sections

^{97}Zr, ^{97}Nb γ ray spectroscopy

^{97}Nb, ^{97}Mo energy levels

1. Introduction

Zirconium is useful as a neutron flux monitor because of its extreme sensitivity to epithermal neutrons (Simonits *et al*., 1987; Khoo *et al*., 2007; Brockman and Robertson, 2009). In capture by ^{96}Zr, the resonance integral is more than two orders of magnitude larger than the thermal cross section, while in capture by ^{94}Zr the ratio is less than one order of magnitude; thus the two isotopes provide a nice contrast in sensitivity to epithermals. Unfortunately there is rather poor agreement in the literature on the values of the thermal cross sections and resonance integrals, with results of activation measurement varying by more than 25% for the ^{94}Zr thermal cross section and the ^{96}Zr resonance integral, while the reported values for the ^{94}Zr resonance integral and the ^{96}Zr thermal cross section vary by more than a factor of 2.

The present work presents a new set of measurements of the Zr cross sections, with particular emphasis on separate and independent measurements of the thermal and epithermal cross sections at different irradiation sites in the reactor. The results reveal significant differences in the resonance integrals at different irradiation sites, which emphasizes the necessity of correcting a thermal cross section measurement for the epithermal neutrons using a resonance integral determined at the same site.

Observation of the irradiated Zr samples also yielded a new set of results on the energy and intensity of the γ rays emitted by ^{97}Zr and its radioactive daughter ^{97}Nb. The present report

presents the results of these measurements, including deduced energies of the excited states of ^{97}Nb and ^{97}Mo and the intensities of the β transitions populating those states.

2. Experimental details

The irradiated samples were Zr metal foil of natural isotopic abundance with masses ranging from 10 to 30 mg and thickness 0.127 mm. In all five different irradiation sites in the Oregon State University TRIGA reactor were used: two in the central core (one of which is lined with Cd to absorb thermal neutrons), two at the outer core (one of which was the fast pneumatic transfer facility or "rabbit"), and a thermal column about 2 m from the central core where the neutrons have an approximately Maxwellian distribution. Some of the samples irradiated in the rabbit facility were enclosed in Cd boxes of 1-mm wall thickness to isolate the epithermal component. All Zr irradiations were accompanied by samples of Au and Co (as dilute impurities in aluminum foils) which served to measure the neutron flux. Thermal fluxes (and epithermal-to-thermal ratios) were typically as follows: central core – 8×10^{12} neutrons cm^{-2} s^{-1} (0.14); outer core - 4×10^{12} neutrons cm^{-2} s^{-1} (0.10); rabbit - 1×10^{13} neutrons cm^{-2} s^{-1} (0.03); thermal column - 7×10^{10} neutrons cm^{-2} s^{-1} (0.003). Measurements were made both before and after the original high-enriched uranium (HEU) reactor fuel was replaced with low-enriched uranium (LEU) fuel.

For the cross section measurements, sample activities ranged from 0.1-1 kBq of ^{95}Zr and 1-10 kBq of ^{97}Zr for the thermal column and rabbit irradiations and from 10-100 kBq of ^{95}Zr and 1-10 MBq of ^{97}Zr for the core irradiations. Spectroscopy samples typically began with 0.5-3 MBq of ^{97}Zr. Some spectroscopy samples were counted initially at a distance of 20 cm from the detector and then after each half-life of decay they were moved closer so as to keep the counting rates approximately uniform, ending at a distance of 5 cm. This enabled peaks due to coincidence

summing to be identified. The spectroscopy samples also contained small amounts of ^{175}Hf, ^{181}Hf, ^{182}Ta, and ^{187}W.

The γ rays were observed with high-resolution Ge detectors (nominal volume of 169 cm^3, efficiency of 35% compared with NaI at 1332 keV, resolution of 1.68 keV at 1332 keV) connected to a digital spectroscopy system. Efficiency calibrations were done with sources of ^{56}Co, ^{133}Ba, and ^{152}Eu using intensities given by Meyer (1990), Trzaska (1990), and Baglin *et al.* (2002). The Ba and Eu sources were used for absolute efficiency calibrations; their activities were certified against standards (provided by the U.S. National Institute of Standards and Technology) to within 0.5%. Below 200 keV, the determination of relative efficiency was augmented using sources of ^{160}Tb, ^{169}Yb, and ^{182}Ta. This gave a total of 36 data points below 444 keV, which were fit using a 4th order polynomial for the logarithmic dependence of efficiency on energy. Above 444 keV the logarithmic dependence is well fit with a linear function.

Energy calibrations were done by counting the Zr samples together with samples of ^{56}Co, ^{56}Mn, ^{133}Ba, ^{152}Eu, and ^{207}Bi and using the γ-ray energies recommended by Helmer and van der Leun (2000). The spectroscopy data were analyzed for peak locations and areas using the fitting code SAMPO (Aarnio *et al.*, 1988).

For the presently deduced relative intensities in the spectroscopy measurements, a minimum uncertainty has been adopted of 2% for energies below 200 keV and 1% above 200 keV. These limits are slightly larger than the optimum uncertainty limits on absolute intensities suggested by Debertin and Helmer (1988) but represent a more realistic estimate that includes both the fitting

uncertainty in our efficiency calibrations and the uncertainty in the activity of our calibration sources. For relative efficiencies needed for the cross section determinations, such limits are rather generous.

For the stronger lines (typically those with more than 10^4 counts in the peak) the fitting and calibration uncertainties often combine to give a net energy uncertainty smaller than 10 eV. This likely exceeds the level of systematic uncertainties, and so the minimum energy uncertainty has been set at 10 eV for peaks whose energies are calibrated directly against the standards. Weaker peaks were analyzed from long counting runs without the calibration standards, so their energy uncertainties are corresponding larger because they are calibrated against other ^{97}Zr lines rather than against the standards.

For the measurements of the cross sections, end-of-bombardment activities were determined from the peak areas by correcting for γ-ray branching and detector efficiency. The activity a then depends on the cross sections according to

$$a = N(\sigma\phi_{\mathrm{th}} + I\phi_{\mathrm{epi}})(1 - e^{-\lambda t_{\mathrm{i}}}) \qquad (1)$$

where N (assumed to be constant) is the number of stable Zr target nuclei in the irradiated sample, ϕ_{th} and ϕ_{epi} are the thermal and epithermal neutron fluxes, σ and I are respectively the effective thermal cross section and resonance integral, and t_{i} is the irradiation time.

Because there are no broad or low-lying neutron resonances known for any of the Zr isotopes considered in the present work, the cross section closely follows the 1/*v* behavior below about 1 eV. Therefore the effective thermal cross section characterizes the entire thermal region. (This is equivalent to setting Wescott's *G* factor equal to 1.0.) The effects of thermal neutron absorption within the samples are also negligible, given the thin samples used in the present experiments. A small correction is necessary to account for absorption of epithermal neutrons in the samples, amounting to about 1.7% for ^{94}Zr and 2.7% for ^{96}Zr (Simonits *et al.*, 1987).

The effective resonance integral *I* includes a small contribution from the 1/*v* region. Assuming the Cd cut-off energy to be about 0.5 eV, this contribution amounts to about 0.45σ; so the corrected resonance integral I' is then (Mughabghab, 2006)

$$I' = I - 0.45\sigma \qquad (2)$$

Because the resonance integral is 1-2 orders of magnitude larger than the thermal cross section for the Zr isotopes, this correction is small – less than one standard deviation of the resonance integral.

The uncertainties in the cross sections include a number of contributions: decay half-lives, γ ray branching ratios, quantity of material, and neutron flux. The currently recommended values of the isotopic abundances are 17.38 ± 0.28 % for ^{94}Zr and 2.80 ± 0.09 % for ^{96}Zr (Berglund and Wieser, 2011). The decay properties have been recently summarized in the Nuclear Data Sheets (NDS) for ^{95}Zr (Basu *et al.*, 2010) and ^{97}Zr (Nica, 2010). The present consensus values of the

half-lives and branching ratios are: ^{95}Zr – 64.032 ± 0.006 d; 44.27 ± 0.22 % (724.2 keV) and 54.38 ± 0.22 % (756.7 keV) and ^{97}Zr – 16.749 ± 0.008 h; 93.09 ± 0.16 % (743.4 keV). The half-lives and branching ratios thus contribute negligibly to the uncertainty budget. The isotopic abundances contribute uncertainties of respectively 1.6 % and 3.2 %. The uncertainties in the flux determinations depend in part on the cross sections of the flux monitors Au (σ = 98.65 ± 0.09 b, I = 1550 ± 28 b) and Co (σ = 37.18 ± 0.06 b, I = 74 ± 2 b), using values from the compilation of Mughabghab (2006). The uncertainties of approximately 2 % in the resonance integrals of the flux monitors correspondingly contribute to the uncertainties in the Zr resonance integrals. Uncertainties in the measurements due to counting statistics are negligible. In the above discussion and in the subsequent presentation of the results of the present measurements, all uncertainties are quoted as one standard deviation.

3. Cross sections

The presently measured cross sections for ^{94}Zr and ^{96}Zr are shown in Tables 1 and 2, along with representative values from the literature for comparison. A noteworthy feature of the present results is the variation in the resonance integral measured at two different sites in the reactor, one in the central core and the other in the periphery. The differences are clearly isotope dependent, yielding a ratio of resonance integrals at the two sites of 1.18 for ^{94}Zr and 1.05-1.08 for ^{96}Zr.

Because of the small thermal cross sections, the deduced value is very sensitive to the correction for the effects of epithermals, and indeed the good agreement in the deduced thermal cross sections at the different sites is dependent on calculating the correction using the resonance integral determined at that site. Otherwise, the thermal cross section would deviate from the tabulated values by 20-30% in ^{94}Zr and by more than a factor of 2 in ^{96}Zr. The exception is in the case of the thermal column measurements, in which there is only a weak sensitivity to the resonance integral: changing from the central core resonance integral to the periphery value changes the deduced value of the ^{94}Zr thermal cross section by a small fraction of a per cent and that of the ^{96}Zr thermal cross section by about 2%, both well within the measurement uncertainty. So even though the resonance integral was not measurable at the thermal column site, its exact value makes a negligible difference in the deduced thermal cross section at that site.

The resulting values of the thermal cross sections at the four reactor sites are then in excellent agreement with one another. The unweighted average of the presently measured values of the

^{94}Zr thermal cross section is 0.0475 ± 0.0012 b, in good agreement with the consensus value of 0.0494 ± 0.0017 b recommended by Mughabghab (2006) and in reasonably good agreement with the previously measured values listed in Table 1.

The unweighted average of the presently measured values of the ^{96}Zr thermal cross section is 0.0210 ± 0.0011 b; owing to the extreme sensitivity of the deduced thermal cross section to the value of the resonance integral, the smallest uncertainties are obtained from the measurements in the thermal column where the relative contribution of the epithermal neutrons to the total flux is smallest. The present value agrees with Mughabghab's recommended value of 0.0229 ± 0.0010 b and also with most of the previously measured values.

4. Gamma-ray spectroscopy

Fig. 1 shows a sample γ-ray spectrum from the decay of an irradiated Zr sample. The nuclide ^{97}Zr decays to ^{97}Nb with a half-life of 16.75 h, and ^{97}Nb decays in turn to stable ^{97}Mo with a half-life of 72.1 min. Owing to the shorter half-life of the ^{97}Nb, the radioactive decay reaches secular equilibrium during the irradiation and subsequent storage time; as a result the γ radiations from the ^{97}Nb decay appear to decay with the 16.75-h half-life of ^{97}Zr, and so it is not possible to use the half-life difference to separate the radiations from the two decays.

The most prominent features in the spectrum of Fig. 1 are the intense 743.4-keV line (93.1%) emitted in the ^{97}Zr decay and 658.2-keV line (98.2%) from the ^{97}Nb decay. Also visible are the much weaker 724.192- and 756.725-keV lines from the ^{95}Zr decay; the energies of these lines have been determined to an uncertainty of the order of 10 eV or less (Basu *et al*., 2010), and so they can serve as additional energy calibrations.

4.1 ^{97}Zr decay

Table 3 shows the energies and intensities of the γ rays from the ^{97}Zr decay observed in the present work compared with the previous consensus values from the NDS (Nica, 2010). The NDS decay data are derived primarily from the singles and coincidence results of Siivola and Graeffe (1968), with additional singles data from Arad *et al*. (1970) and singles, coincidence, and β spectrum results from Megli *et al*. (1970). The present results show an improvement over the previous data in the reduction of the uncertainties in both energy and intensity by typically an

order of magnitude. In addition, small upper limits have been set on several of the lines that have been previously reported but not placed in the ^{97}Nb level scheme. All of the transitions listed in Table 3 have been checked for agreement with the 16.75-h half-life of ^{97}Zr.

Based on the energies and intensities of the γ radiations shown in Table 3, the ^{97}Nb energy levels and β feeding intensities shown in Table 4 have been deduced. Of the 33 γ rays listed in Table 3 that have been placed in the ^{97}Nb level scheme, 19 fit their proposed placements within 1 standard deviation and 29 fit within 2 standard deviations, which matches the expected statistical distribution and suggests that the transition and level uncertainties have been neither over- nor underestimated. The single exception is the 558.2-keV transition, which despite its small intensity and large energy uncertainty (110 eV) still misses the energy difference of its previously suggested placement more than 6 standard deviations. No other placement among the known levels offers a better match.

Also among the γ rays listed in Table 3 are several previously known but unplaced transitions: 294.6, 408.5, and 1110.4 keV. None of these transitions can be fit among the known levels of ^{97}Nb, which suggests that there are additional as yet unidentified levels populated in the decay of ^{97}Zr. The present fits to the line at 1362.7 keV do not show evidence for doublet structure, and so the second line in that region at 1361.0 keV listed by the NDS appears not to be part of the ^{97}Zr decay.

The spectra show an unresolved triplet of lines around 804 keV. The more intense members of the triplet have been previously assigned to the decay of ^{97}Zr but not placed in the decay scheme.

Based on the present results, the highest energy member of the triplet fits nicely between the levels at 1548.6 and 743.4 keV and so that placement is tentatively proposed in Table 3. The most intense member of the triplet (804.4 keV) cannot be placed among the presently known levels of ^{97}Nb populated in the ^{97}Zr decay. The third member of the triplet, 802.4 keV, has not been previously reported in either the ^{97}Zr or ^{97}Nb decays.

4.2 ^{97}Nb decay

Table 5 lists the energies and intensities of the γ rays observed in the present work in the decay of ^{97}Nb to levels in ^{97}Mo in comparison with the NDS values. The latter are based on the γ-ray singles and coincidence experiments previously reported by Graeffe and Siivola (1968), with additional singles data reported by Singh *et al*. (1969) and Arad *et al*. (1970). As was the case with the ^{97}Zr decays, the present data have reduced the uncertainties in energy and intensity by typically an order of magnitude. All of the γ rays listed in Table 5 appear to decay with the 16.75-h half-life characteristic of the parent ^{97}Nb. The correspondingly deduced energy levels and β feedings of the states in ^{97}Mo are shown in Table 6.

The transitions at 177.2 and 238.5 keV were previously observed in decay studies but not placed in the decay scheme. A level at 480.9 keV appeared in several previous nuclear reaction studies of ^{97}Mo, including He,xn reactions (Mesko *et al*., 1972; Carnes *et al*., 1987), neutron capture (Demidov *et al*., 1974), inelastic neutron scattering (Abbondanno *et al*., 1989), and Coulomb excitation (Barrette *et al*., 1975). The 480.9-keV γ ray observed in the present work is presumably the ground-state transition from this level, which has not been reported in previous

decay studies. This 3/2+ excited state cannot be populated directly from the β decay of the 9/2+ ^{97}Nb, but several transitions appear to be excellent energy fits to other excited states that can lead to the 480.9-keV level, including not only the aforementioned 177.2- and 238.5-keV γ rays respectively from the levels at 658.2 and 719.3 keV, but also that at 787.6 keV (from the level at 1268.5 keV). The previously reported but unplaced transition at 1148.6 keV could possibly connect the level at 1629.2 keV with the 480.9-keV level; however, due to the strong transition at 1148.1 keV in the ^{97}Zr decay, this transition in the ^{97}Nb decay could not be seen in the present work.

A γ ray of energy 679.6 keV observed in the present work has not been reported in previous decay studies but is well known from reaction studies as the ground-state transition from a 1/2+ state at that energy. This state also cannot be directly populated in the β decay of ^{97}Nb, and no transitions in the decay appear to populate that state from higher-lying excited states, so the present identification should be regarded as tentative. It is possible that the 1/2+ state is populated by a very weak β branch from the 1/2-, 59-s isomeric state at 743.4 keV in ^{97}Nb. The log *ft* for such a transition would be 7.63, which is in the correct range for a first-forbidden transition, so such a hypothesis is not unreasonable.

The levels at 721.0 and 1409.6 keV are also new to the radioactive decay scheme but are well known from the previous nuclear reaction studies. The former level is identified through its ground-state transition and the latter through the 751.4-keV transition to the 658.2-keV level.

An unresolved triplet of lines appears around 910 keV. Two components of this triplet, at 908.5 and 909.9 keV, probably connect the level at 1629.3 keV with the doublet at 721 keV. The upper member of the triplet is the background line at 911.2 keV, whose intensity was comparable to the other 2 members. As the sample aged, the energies of the lines became distorted and their intensities relative to 658.2 keV increased, probably due to the relative growing in of yet another component. When the samples were allowed to decay so that the ^{97}Zr activity was negligible, this new activity was identified as 78-h ^{89}Zr, presumably formed by (n,2n) reactions on ^{90}Zr.

With the newly placed γ rays included in the decay scheme, the energies of 13 of the 20 placed transitions in Table 5 match their placements within 1 standard deviation and 19 match within 2 standard deviations, which suggests a satisfactory statistical distribution.

4.3 Unplaced γ rays

Table 7 shows 9 additional γ rays that appear to follow the decay of ^{97}Zr. All were observed from each of the 5 samples counted in the present experiments, none is associated with any identified background or impurity activity, and all appeared with uniform intensity at source-to-detector distances ranging from 5 to 20 cm, making it unlikely that the lines are due to coincidence summing. The 4 lowest energy lines in Table 7 occur on large time-dependent backgrounds from Compton events associated with 658.2 and 743.4 keV, so their time dependences could not be unambiguously analyzed. However, owing to the greater peak-to-background ratios above 743 keV, the decay with time of the 5 highest energy lines could be determined to follow the expected 16.75-h decay of the ^{97}Zr. The present data do not permit a determination of which decay produces these radiations, and indeed none of them can be fit among the known levels of

either ^{97}Nb or ^{97}Mo. None of these lines have been reported in any of the previous ^{97}Zr decay studies, but they are too weak to have appeared in the previously measured spectra. Singh *et al*. (1969) and Arad *et al*. (1970) reported γ-ray spectra from the ^{97}Nb decay using samples free of ^{97}Zr, the former having produced their samples through photoreactions and the latter performing chemical separations on neutron-activated Zr to extract the Nb activity. Based on their reported spectra, it can be concluded that if the 802.4, 1201.9, and 1298.0 keV lines were emitted in the ^{97}Nb decay they should have been visible in the spectra of Arad *et al*. and similarly for the 1166.8 and 1298.0 keV lines in the spectra of Singh *et al*. If these 4 lines are indeed part of this decay sequence they are probably associated with the ^{97}Zr rather than the ^{97}Nb decay.

5. Discussion

The measurements of the thermal cross sections in the present work demonstrate the importance of careful correction for the effect of epithermal neutrons, and in particular the necessity of correcting for the epithermals using a resonance integral measured at the same site. The extreme sensitivity of the ^{96}Zr thermal cross section to the epithermal correction provides a convincing demonstration of this effect. The variation in the resonance integral at different sites in our reactor is clearly an isotope-dependent effect, more extreme in the present experiments for ^{94}Zr than for ^{96}Zr. The resonance integral is defined as

$$I = \int_{E_{Cd}}^{\infty} \frac{\sigma(E)}{E} dE \qquad (3)$$

where the cadmium cut-off energy E_{Cd} is generally assumed to be about 0.5 eV. Here the epithermal flux is assumed to vary like E^{-1} over the resonance region (roughly 1 eV to 100 keV), and the calculation requires complete information on the properties of the resonances. However, the energy dependence of the epithermal flux often deviates from this assumed behavior and can be characterized instead as $E^{-(1+\alpha)}$, where α is a small parameter, typically between -0.1 and +0.1 (Khoo *et al.*, 2007). If the epithermal flux shows different energy dependences at different reactor sites, it should not be surprising that (depending on the distribution of resonances across the epithermal region) evaluating the resonance integral from eq. 3 will give different results at different sites, and furthermore that the effect will be nuclide dependent owing to differing sets of resonance parameters. Indeed, we have seen a similar effect with the 7 of the 8 radioisotopes

produced in the irradiation of Cd, with ratios of resonance integrals measured in the central core and outer core ranging from 1.1 to 1.8 for the various isotopes (Gicking 2011). Nevertheless, despite the variation at different reactor sites, the measured Zr resonance integrals are overall in rough agreement with those calculated from the known resonance parameters according to Mughabghab (2006) – 0.265 ± 0.015 b for ^{94}Zr and 5.15 ± 0.26 b for ^{96}Zr.

The present work has also resulted in considerable improvements in the spectroscopy of the ^{97}Zr and ^{97}Nb decays, including the suggested placement into the level scheme of several γ rays newly observed in the decays. Nevertheless, several moderately intense transitions remain unplaced in the ^{97}Zr decay. Because most of the β decay intensity is concentrated in a single branch, unplaced γ transitions even of low intensity may have a relatively significant effect on the analysis of the remaining weak β branches. For example, the NDS compilation (Nica, 2010) discusses the problems with the ^{97}Zr β branches leading to the 5/2+ states at 1750.5 and 1851.7 keV in ^{97}Nb. These β transitions would be of the unique second forbidden type, for which one would expect a log *ft* value of at least 11, in contrast to the values of about 8.3 deduced on the basis of the previous decay scheme. The present results have reduced the intensity of the β branch to the 1750.5 keV level by half and that to the 1851.7 keV level to 0 within statistics. However, there remains sufficient unplaced γ ray intensity in the ^{97}Zr decay to make significant alterations in these conclusions, and so the β intensities and deduced log *ft* values should be regarded as provisional. Indeed, the 0.23% β branch to the 1750.5 keV level more likely suggests additional unidentified γ intensity of that amount leading to the level than it does an extreme outlier in the systematics of log *ft* values.

Acknowledgements

The assistance of and support by the reactor staff of the Oregon State University Radiation Center in performing the irradiations is acknowledged with appreciation.

References

Aarnio, P. A., Routti, J. T., Sandberg, J. V., 1988. MicroSAMPO – Personal computer based advanced gamma spectrum analysis system. J. Radioanal. Nucl. Chem. 124**,** 457-465.

Annondanno, U., Demanins, F., Raicich, F., 1989. A study of the ^{97}Mo(n, n'γ)^{97}Mo reaction. Nuovo Cim. 102A, 1533-1562.

Arad, B., Prestwich, W. V., Lopez, A. M., Fritze, K., 1970. Decay of ^{97}Zr and its daughter ^{97}Nb. Can. J. Phys. 48, 1378-1385.

Baglin, C. M., Browne, E., Norman, E. B., Molnár, G. L., Belgya, T., Révay, Zs., Szelecsényi, F., 2002. ^{66}Ga: a standard for high-energy calibration of Ge detectors. Nucl. Inst. Meth. Phys. Res. A 481, 365-377.

Barrette, J., Barrette, M., Haroutunian, R., Lamoureux, G., Monaro, S., 1975. Coulomb excitation of levels in ^{95}Mo and ^{97}Mo. Phys. Rev. C 11, 171-187.

Basu, S. K., Mukherjee, G., Sonzogni, A. A., 2010. Nuclear data sheets for A = 95. Nucl. Data Sheets 111, 2555-2737.

Berglund, M., Wieser, M. E., 2011. Isotopic compositions of the elements 2009. Pure Appl. Chem. 83, 397-410.

Brockman, J. D., Robertson, J. D., 2009. Analysis of k_0 neutron activation analysis at the University of Missouri Research Reactor. Applied Radiation and Isotopes 67, 1084-1088.

Carnes, K. D., Rickey, F. A., Samudra, G. S., Simms, P. C., 1987. Particle-core multiplets in ^{97}Mo populated via the (^{3}He,2nγ) reaction. Phys. Rev. C 35, 525-533.

Debertin, K., Helmer, R. G., 1988. Gamma- and x-ray spectrometry with semiconductor detectors. Elsevier, Amsterdam.

Demidov, A. M., Akhmed, M. R., Khalil, M. A., Al-Nazar, S., 1974. γ-ray spectra from thermal-neutron capture in ^{96}Mo, ^{98}Mo, and ^{100}Mo. Izv. Akad. Nauk SSSR, Ser. Fiz. 37, 998-1003. Transl.: Bull. Acad. Sci. USSR, Phys. Ser. 37, No. 5, 74-78.

Fulmer, R. H., Stricos, D. P., Ruane, T. F., 1971. Neutron absorption cross sections for zirconium-94 and zirconium-96. Nucl. Sci. & Eng. 46, 314-317.

Gicking, A., 2011. Neutron capture cross section of cadmium isotopes. Thesis, Oregon State University (unpublished).

Graeffe, G., Siivola, A., 1968. The decay of ^{97}Nb. Nucl. Phys. A 109, 380-384.

Heft, R. E., 1978. A consistent set of nuclear-parameter values for absolute INAA. Proceedings of the Conference on Computers in Activation Analysis, ed. by R. Farmakes, American Nuclear Society, La Orange Park, IL, pp. 495-510.

Helmer, R.G., van der Leun, C., 2000. Recommended standards for γ-ray energy calibration (1999). Nucl. Instr. Meth. Phys. Res. A 450, 35-70.

Khoo, K. S., Sarmani, S. B., Abugassa, I. O., 2007. Determination of thermal to epithermal neutron flux ratio (f), epithermal neutron flux shape factor (α) and comparator factor (F_c) in the Triga Mark II Reactor, Malaysia. J. Radioanal. Nucl. Chem. 271, 419-424.

Megli, D. G., Agin, G. P., Potnis, V. R., Mandeville, C. E., 1970. Decay of ^{97}Zn to nuclear states of ^{97}Nb. Z. Physik 234, 95-106.

Mesko, L., Nilsson, A., Hjorth, S. A., Brenner, M., Holmlund, O., 1972. High-spin levels in ^{95}Mo and ^{97}Mo from (α,xn) reactions. Nucl. Phys. A 181, 566-588.

Meyer, R. A., 1990. Multigamma-ray calibration standards. Fizika 22, 153-182.

Mughabghab, S. F., 2006. Atlas of Neutron Resonances, 5th ed., Elsevier, Amsterdam.

Nakamura, S., Furutaka, K., Harada, H., Katoh, T., 2003. Thermal neutron capture cross sections and resonance integrals of ^{80}Se, ^{94,96}Zr, and ^{124}Sn. Report no. INDC(JPN)-190/U, Japan Atomic Energy Research Institute, p. 26.

Nica, N., 2010. Nuclear data sheets for A = 97. Nucl. Data Sheets 111, 525-716.

Prajapati, P. M., et al., 2012. Measurement of neutron-induced reaction cross sections in zirconium isotopes at thermal, 2.45 MeV and 9.85 MeV energies. Nucl. Sci. & Eng. 171, 78-84.

Ricabarra, M. D., Turjanski, R., Ricabarra, G. H., 1970. Anomalous ^{96}Zr resonance integral to thermal activation cross-section ratio and the neutron activation resonance integral of ^{94}Zr and ^{96}Zr. Can. J. Phys. 48, 2362-2370.

Santry, D. C., Werner, R. D., 1973. Thermal neutron activation cross sections and resonance integrals of ^{94}Zr and ^{96}Zr. Can. J. Phys. 51, 2441-2443.

Siivola, A., Graeffe, G., 1968. The decay of ^{97}Zr. Nucl. Phys. A 109, 369-379.

Simonits, A., De Corte, F., De Wispelaere, A., Hoste, J., 1987. Nuclear data measurements for zirconium isotopes used for activation analysis and neutron metrology. J. Radioanal. Nucl. Chem. 113, 187-197.

Singh, B., Cox, R. J., Kukoč, A. H., King, J. D., Taylor, H. W., 1969. A study of the gamma rays emitted by ^{97}Nb. Nucl. Phys. A 129, 104-112.

Trzaska, W. H., 1990. Recommended data on selected gamma-ray and conversion-electron calibration sources. Nucl. Inst. Meth. Phys. Res. A 297, 223-229.

Van der Linden, R., De Corte, F., Van den Winkel, P., Hoste, J., 1972. A compilation of infinite dilution resonance integrals, I. J. Radioanal. Chem. 11, 133-141.

Wyrick, J. M., Poenitz, W. P., 1982. Neutron-capture-activation cross sections of ^{94,96}Zr and ^{98,100}Mo at thermal and 30 keV energy. Argonne National Laboratory report no. 83-4, 196-204.

Xiao-Long, H., Xiao-Gang, H., Wei-Xiang, Y., Han-Lin, L., Wen-Rong, Z., 2000. Measurements of thermal neutron capture cross section. Atomic Energy Sci. & Tech. 34, 456-459.

Figure caption

Fig. 1. Gamma-ray spectrum from the decay of irradiated Zr, showing prominent peaks from the decays of ^{97}Zr and its daughter ^{97}Nb. Other marked peaks include those due to coincidence summing (Σ), background (B), and newly identified peaks (N) that may be associated with these decays.

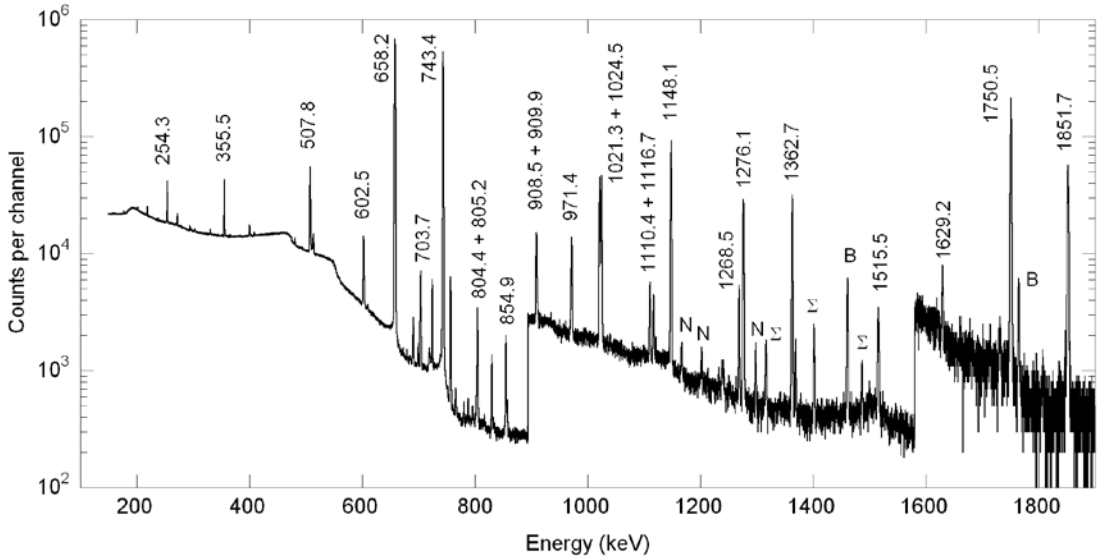
Counts per channel
Energy (keV)
254.3
355.5
507.8
602.5
658.2
703.7
743.4
804.4 + 805.2
854.9
908.5 + 909.9
971.4
1021.3 + 1024.5
1110.4 + 1116.7
1148.1
1268.5
1276.1
1362.7
1515.5
1629.2
1750.5
1851.7
B
N

Table 1. Neutron capture cross sections of ^{94}Zr

		σ (b)	*I* (b)
Present work	Central core	0.0465(14)[a] 0.0493(14)[b]	0.376(14)[a] 0.393(14)[b]
	Outer core	0.0478(12)[a] 0.0485(13)[b]	
	Rabbit	0.0477(11)[a] 0.0469(11)[b]	0.318(12)[a] 0.334(13)[b]
	Thermal column	0.0460(11)[a] 0.0470(11)[b]	
Previous work	Ricabarra (1970)	0.063(8)	0.369(37)[c]
	Fulmer (1971)	0.052(3)	0.30(3)
	Santry (1973)	0.0475(24)	0.218(24)
	Heft (1978)	0.055(2)	0.296(50)
	Wyrick (1982)	0.0499(17)	
	Xiao-Long (2000)	0.053(2)	
	Nakamura (2003)	0.0478(13)	0.278(15)
	Prajapati (2012)	0.051(8)	

[a]HEU fuel
[b]LEU fuel
[c]Reduced resonance integral I', corrected for $1/v$ component

Table 2. Neutron capture cross sections of ^{96}Zr

		σ (b)	*I* (b)
Present work	Central core	0.021(13)[a]	5.52(25)[a] 5.70(26)[b]
	Outer core	0.023(9)[a] 0.022(9)[b]	
	Rabbit	0.021(3)[a] 0.019(4)[b]	5.25(24)[a] 5.26(24)[b]
	Thermal column	0.0201(11)[a] 0.0219(11)[b]	
Previous work	Ricabarra (1970)	0.057(10)	4.79(50)[c]
	Fulmer (1971)	0.020(3)	5.0(4)
	Santry (1973)	0.0229(10)	5.20(34)
	Heft (1978)	0.00(1)	5.98(15)
	Wyrick (1982)	0.0203(6)	
	Nakamura (2003)	0.0438(56)	4.94(100)
	Prajapati (2012)	0.024(4)	

[a]HEU fuel
[b]LEU fuel
[c]Reduced resonance integral I', corrected for $1/v$ component

Table 3. Energies and intensities of γ rays emitted in the decay of ^{97}Zr

Previous work[a]		Present work		Levels[b]
E (keV)	*I*	*E* (keV)	*I*	
111.6(3)	0.070(10)	111.769(14)	0.101(2)	$J \rightarrow H$
182.9(5)	0.034(7)	182.869(38)	0.011(2)	$F \rightarrow D$
202.5(6)	0.031(9)	201.846(24)	0.045(1)	$I \rightarrow G$
218.9(2)	0.18(2)	218.944(10)	0.225(4)	$H \rightarrow F$
254.17(14)	1.23(8)	254.347(10)	1.48(1)	$M \rightarrow K$
272.40(16)	0.25(3)	272.446(10)	0.312(3)	$G \rightarrow E$
294.8(4)	0.09(3)	294.620(18)	0.104(3)	
297.2(3)	0.071(12)	297.331(34)	0.051(2)	$G \rightarrow D$
305.1(9)	0.03(2)	303.060(23)	0.057(2)	$K \rightarrow G$
330.43(19)	0.154(16)	330.713(18)	0.122(1)	$J \rightarrow F$
355.40(9)	2.25(10)	355.549(10)	2.47(2)	$M \rightarrow I$
400.42(16)	0.263(17)	400.610(10)	0.326(3)	$G \rightarrow C$
410(1)	0.07(5)	408.473(25)	0.089(2)	
473.5(6)	0.08(4)	474.413(22)	0.059(2)	$I \rightarrow E$
507.64(8)	5.4(2)	507.805(10)	5.76(6)	$D \rightarrow B$
513.41(18)	0.59(5)	513.551(10)	0.613(6)	$J \rightarrow D$
558(1)	0.03(2)	558.20(11)	0.010(2)	$M \rightarrow G$
600.6(6)	<0.2	600.466(39)	0.021(2)	$K \rightarrow D$
602.37(14)	1.48(8)	602.493(10)	1.57(2)	$I \rightarrow C$
		672.137(36)	0.023(2)	$M \rightarrow F$
690.52(16)	0.197(19)	690.611(10)	0.297(3)	$F \rightarrow B$
699.2(3)	0.108(21)	698.948(10)	0.103(1)	$N \rightarrow G$
703.76(5)	1.09(5)	703.692(10)	1.07(1)	$K \rightarrow C$
707.4(6)	0.034(18)	705.159(21)	0.115(2)	$L \rightarrow D$
743.36(3)	100	743.402(10)	100(1)	$B \rightarrow A$
772(3)	0.26(14)		<0.001	
775.0(8)	0.29		<0.005	
804.52(9)	0.66(8)	804.414(25)	0.51(2)	
805.6(8)	0.30	805.153(46)	0.18(2)	$G \rightarrow B$
829.79(9)	0.257(19)	829.921(10)	0.230(2)	$M \rightarrow E$
854.89(8)	0.383(24)	854.923(10)	0.373(4)	$M \rightarrow D$
971.34(15)	0.299(18)	971.442(10)	0.302(3)	$N \rightarrow E$
1018.1(8)	0.40		<0.001	
1021.2(3)	1.09(18)	1021.328(10)	1.20(1)	$J \rightarrow B$
1026.7(8)	0.30		<0.001	
1110.44(19)	0.10(2)	1110.403(15)	0.134(2)	
1147.97(8)	2.81(11)	1148.053(10)	2.78(3)	$C \rightarrow A$
1276.07(9)	1.01(6)	1276.142(10)	1.01(1)	$E \rightarrow A$
1361.0(8)	0.7			
1362.68(9)	1.10(11)	1362.658(10)	1.15(1)	$M \rightarrow B$
1750.24(22)	1.17(11)	1750.507(10)	1.04(2)	$I \rightarrow A$
1851.61(9)	0.33(3)	1851.719(12)	0.318(6)	$K \rightarrow A$
2203(2)			<0.001	

[a]From Nuclear Data Sheets (Nica, 2010).
[b]See Table 4 for level designations.

Table 4. Energy levels of ^{97}Nb populated in the decay of ^{97}Zr

Level label	Previous work[a]				Present work		
	E (keV)	J^{π}	I_{β} (%)	Log ft	E (keV)	I_{β} (%)	Log ft
A	0.000	$9/2^{+}$			0.000		
B	743.35(3)	$1/2^{-}$	87.8(4)	7.227(3)	743.405(10)	87.2(1)	7.230(2)
C	1147.96(6)	$7/2^{+}$			1148.048(7)		
D	1251.01(7)	$3/2^{-}$	3.90(20)	8.046(23)	1251.202(11)	4.27(8)	8.007(9)
E	1276.09(7)	$5/2^{+}$	0.12(8)	9.5(3)	1276.151(10)	0.10(2)	9.61(9)
F	1433.92(13)	$5/2^{-}$			1434.019(14)	<0.02	>10.8
G	1548.36(11)	$(3/2^{+},5/2^{-})$	0.36(5)	8.68(6)	1548.633(9)	0.61(2)	8.455(15)[b]
H	1652.82(21)		0.102(21)	9.07(9)	1652.963(17)	0.116(4)	9.014(16)
I	1750.43(9)	$5/2^{+}$	0.46(17)	8.25(16)	1750.532(8)	0.23(4)	8.55(8)
J	1764.42(14)	$(3/2^{-})$	1.77(18)	7.64(5)	1764.744(9)	1.90(4)	7.61(1)
K	1851.71(6)	$5/2^{+}$	0.27(11)	8.29(18)	1851.740(8)	<0.03	>9.2
L	1958.4(6)		0.032(17)	9.00(23)	1956.364(72)	0.107(3)	8.479(13)
M	2105.91(6)	$(3/2^{+})$	4.95(17)	6.448(16)	2106.095(7)	5.4(1)	6.409(10)
N	2247.46(15)	$3/2^{-}$	0.38(3)	7.12(4)	2247.590(10)	0.378(8)	7.125(12)

[a]From Nuclear Data Sheets compilation (Nica, 2010).
[b]Log ft calculated assuming $3/2^{+}$ assignment. If $5/2^{-}$, log ft = 9.089(15).

Table 5. Energies and intensities of γ rays emitted in the decay of ^{97}Nb

Previous work[a]		Present work		Levels[b]
E (keV)	*I*	*E* (keV)	*I*	
178.0(3)	0.05(1)	177.230(21)	0.044(1)	$C \rightarrow B$
238.4(3)	0.05(1)	238.472(21)	0.026(1)	$E \rightarrow B$
		366.359(11)	0.042(1)	$G \rightarrow C$
		480.926(21)	0.187(2)	$B \rightarrow A$
549.25(20)	0.05(1)	549.104(24)	0.055(2)	$I \rightarrow E$
657.94(9)	100	658.178(10)	100(1)	$C \rightarrow A$
		679.554(10)	0.042(1)	$D \rightarrow A$
719.53(19)	0.092(9)	719.334(20)	0.074(2)	$E \rightarrow A$
		721.017(31)	0.039(1)	$F \rightarrow A$
		751.370(27)	0.014(1)	$J \rightarrow C$
		787.570(10)	0.041(1)	$I \rightarrow B$
		796.215(12)	0.024(1)	$K \rightarrow E$
857.46(21)	0.046(7)	857.356(21)	0.044(1)	$K \rightarrow C$
909.55(14)	0.041(7)	908.466(54)	0.030(2)	$L \rightarrow F$
		909.871(67)	0.023(2)	$L \rightarrow E$
1024.4(3)	1.11(7)	1024.519(10)	1.10(1)	$G \rightarrow A$
1117.02(18)	0.087(8)	1116.672(23)	0.089(1)	$H \rightarrow A$
1148.6(3)	0.05(1)			$L \rightarrow B$
1268.62(10)	0.15(2)	1268.472(12)	0.152(2)	$I \rightarrow A$
1515.66(19)	0.124(13)	1515.471(12)	0.113(1)	$K \rightarrow A$
1629.09(22)	0.025(7)	1629.227(46)	0.022(1)	$L \rightarrow A$

[a]From Nuclear Data Sheets (Nica, 2010).
[b]See Table 6 for level designations.

Table 6. Energy levels of ^{97}Mo populated in the decay of ^{97}Nb

Level label	Previous work[a]				Present work		
	E (keV)	J^{π}	I_{β} (%)	Log ft	E (keV)	I_{β} (%)	Log ft
A	0.000	$5/2^+$			0.000		
B	480.91(6)	$3/2^+$			480.917(11)		
C	658.13(5)	$7/2^+$	98.39(9)	5.353(5)	658.180(10)	98.2(1)	5.354(5)
D	679.59(7)	$1/2^+$			679.557(10)		
E	719.20(7)	$5/2^+$	<0.016	>9.1	719.337(22)		
F	720.92(14)	$3/2^+$			720.988(15)		
G	1024.45(8)	$7/2^+$	1.09(7)	6.75(3)	1024.525(10)	1.12(2)	6.743(10)
H	1116.74(8)	$9/2^+$	0.085(8)	7.69(5)	1116.679(23)	0.087(2)	7.683(12)
I	1268.63(8)	$7/2^+$	0.196(22)	7.01(5)	1268.479(9)	0.244(3)	6.914(8)
J	1409.47(11)	$11/2^+$			1409.553(29)	0.014(1)	7.79(4)
K	1515.72(9)	$9/2^+$	0.167(15)	6.38(4)	1515.505(10)	0.178(3)	6.356(11)
L	1629.91(16)	$7/2^+$	0.065(10)	6.34(7)	1629.242(46)	0.111(13)	6.10(6)

[a]From Nuclear Data Sheets compilation (Nica, 2010).

Table 7. Unplaced γ rays possibly following decay of ^{97}Zr or ^{97}Nb

E (keV)	*I* (^{97}Zr norm)	*I* (^{97}Nb norm)
141.632(28)	0.020(1)	0.018(1)
269.653(42)	0.021(2)	0.019(2)
493.595(46)	0.033(2)	0.029(2)
560.320(34)	0.032(2)	0.028(2)
780.480(19)	0.029(1)	0.026(1)
802.421(34)	0.032(2)	0.028(2)
1166.822(22)	0.025(1)	0.022(1)
1201.933(20)	0.024(1)	0.021(1)
1297.958(19)	0.040(1)	0.035(1)